

# Stable Isotope Metabolic Labeling-Based Quantitative Thiol Redox Proteomic Analysis of Hydrogen Peroxide-treated *Arabidopsis* plant

Qin Hu<sup>1</sup>, Guangyu Guo<sup>1</sup>, Zhu Yang<sup>1</sup>, Yaojun Li<sup>1</sup>, Yiji Xia<sup>2</sup> and Ning Li<sup>1\*</sup>

<sup>1</sup>Division of Life Science, the Hong Kong University of Science and Technology, Clear Water Bay, Hong Kong SAR, China

<sup>2</sup>Department of Biology, Hong Kong Baptist University, Kowloon Tong, Hong Kong SAR, China

## Abstract

Homeostasis of protein thiol redox plays an important role in numerous cellular processes and stress responses. The thiol moiety of cysteine residue is easily altered to various redox isoforms that play critical roles in regulation of both structure and function of proteins. In the present study, a quantitative thiol redox proteomic method, termed *OxNSIL*, has been developed, which integrates the chemical labeling by biotin-tagged alkylating reagents with the heavy nitrogen stable isotope-coded salt metabolic labeling and acquires both advantages of biotin-avidin enrichment and MS-based quantitation of cysteine residue-containing peptides. Both the reduced and the reversibly oxidized cysteine thiol moieties are finally identified in a site-specific manner and measured in a single experiment. Hydrogen peroxide, H<sub>2</sub>O<sub>2</sub>, was applied on the whole *Arabidopsis* plant to trigger thiol redox state alteration in order to obtain a proof-of-concept result for application of *OxNSIL* approach in plants. A total of 438 non-redundant biotin-tagged thiol-alkylated peptides representing 391 different cysteine-containing proteins were eventually obtained, among which 17 redox-sensitive biotin tag-labeled peptides were significantly altered by H<sub>2</sub>O<sub>2</sub>. Some well-known ROS-related proteins, such as Ferredoxins 1/2, RuBisCO large subunit, RuBisCO activase, and Fructose-bisphosphate aldolase 6/8 were also detected as the oxidation-sensitive thiol redox proteins. These results substantiate the usefulness of *OxNSIL* approach in study of *in planta* ROS-induced cellular thiol redox state alterations.

**Keywords:** *Arabidopsis thaliana*; Biotin-tagged alkylating chemical labeling; <sup>15</sup>N stable isotope metabolic labeling; *OxNSIL*; Quantitative thiol redox proteomics; Reactive oxygen species (ROS)

**Abbreviations:** ROS: Reactive Oxygen Species; RNS: Reactive Nitrogen Species; *OxNSIL*: <sup>15</sup>N Stable Isotope Metabolic Labeling-Based Thiol Redox Proteomics in *Arabidopsis*; *SILIA*: Stable Isotope Labeling in *Arabidopsis*; PTM: Post-Translational Modification; NEM: N-Ethylmaleimide; IAM: Iodoacetamide; MPB: 3-(N-Maleimido-Propionyl) Biotin; BIAM: N-(Biotinoyl)-N'-(Iodoacetyl)-Ethylendiamine; TCEP: Tris(2-Carboxyethyl) Phosphine; 2DE: 2-Dimensional Gel Electrophoresis; RSB: Re-Suspension Buffer; FDR: False Discovery Rate; *E*-value: Expectation Value; MudPIT: Multidimensional Protein Identification Technology

## Introduction

Reactive oxygen species (ROS) or reactive nitrogen species (RNS) are continuously produced under various conditions [1,2], leading to an imbalance of cellular redox homeostasis [3], which is both physiologically necessary and potentially destructive [4]. Although ROS and RNS are generated in lower amounts within cell under physiological conditions, they play an integral role in modulation of cellular functions including metabolism, gene expression, signal transduction, vasorelaxation, defense against invading pathogens, and so on [5-7]. The major targets of ROS/RNS in living cells are proteins that are capable of scavenging 50~75% of reactive radicals [8], which consequently cause distinct post-translational modifications (PTMs) on proteins [9,10] and further modulate many biological responses [11,12]. Among the protein residues modified during the imbalance of redox states, the sulphur-containing residues, cysteine (Cys) and methionine (Met), are most susceptible to attacks by radicals [9]. The thiol moiety of Cys residue is particularly sensitive to ROS/RNS and can be easily oxidized to various forms, including disulfide (-S-S-), S-nitrosothiols (-SNO), sulfenic acid (-SOH), sulfinic acid (-SO<sub>2</sub>H), and sulfonic acids (-SO<sub>3</sub>H) [13]. The reversible modifications of cysteines, such as -S-S-, -SNO and -SOH, play important roles in protecting

proteins from irreversible damages and modulating the function of proteins [9]. As the homeostasis of thiol-disulfide depends on the redox state of the cells [14,15], quantitative measurement of redox status of certain protein cysteine residues is able to provide useful information on cascades of redox events in a plant cell under a specific stimulation triggered either by an environmental alternation or developmental factor, and eventually to establish redox PTM networks during cellular processes [16].

In contrast to detection of the reversibly oxidized methionine sulphoxide (R-SOCH<sub>3</sub>), which shows a corresponding adducts with a mass shift of 16 Da in mass spectra, the characterization of the redox state of Cys residue is much more challenging because of the difficulty in detection of the oxidized protein cysteines directly. Since both reduced and oxidized forms of thiol group are of relatively high reactivity and the reversibly oxidized forms of protein cysteines have no strong chemical signature, it is practicable to measure the redox status of cysteines through the differentially chemical labeling of the reduced and oxidized forms of these residues. Free -SH (thiol), i.e. the reduced form of cysteine, can react with thiol-reactive reagents easily, such as N-ethylmaleimide (NEM) derivatives [17], iodoacetamide (IAM) derivatives [18], thiol-disulfide exchange reagents [19] and acryloyl derivatives [20]. These alkylating reagents can be conjugated with different tags, such as biotin, fluorochrome, radioactive moieties

**\*Corresponding author:** Ning Li, Division of Life Science, The Hong Kong University of Science and Technology, Clear Water Bay, Hong Kong SAR, China, Tel: +852-23587335; Fax: +852-23581559; E-mail: [boningli@ust.hk](mailto:boningli@ust.hk)

Received April 25, 2014; Accepted May 21, 2014; Published May 26, 2014

**Citation:** Hu Q, Guo G, Yang Z, Li Y, Xia Y, et al. (2014) Stable Isotope Metabolic Labeling-Based Quantitative Thiol Redox Proteomic Analysis of Hydrogen Peroxide-treated *Arabidopsis* plant. J Proteomics Bioinform 7: 121-133. doi:10.4172/0974-276X.1000312

**Copyright:** © 2014 Hu Q, et al. This is an open-access article distributed under the terms of the Creative Commons Attribution License, which permits unrestricted use, distribution, and reproduction in any medium, provided the original author and source are credited.

and chemical entities linked to antibodies to facilitate the purification, detection and/or quantification [21]. To differentiate and quantify the reduced form of protein cysteine at certain redox status, the general method is to alkylate the thiols directly when proteins are isolated from the whole lysates [22,23]. In the case of studying the reversibly oxidized form, thiol-reducing reagent, such as tris(2-carboxyethyl) phosphine (TCEP) or dithiothreitol (DTT), has been frequently applied after free thiols are masked by a thiol-reactive reagent to convert the reversibly oxidized forms, such as disulfide, into free thiol moiety, which are consecutively labeled with another thiol-reactive reagent [24].

In order to investigate protein cysteine redox status, two types of proteomic methods have been frequently used: gel-based and MS-based methods. The gel-based method has been widely applied in distinguishing the differentially post-translation modified proteins, such as redox modification of cysteines [25]. One example is the non-reducing/reducing diagonal 2D-PAGE, which analyzes the global disulfide proteome before the thiol-reactive reagents were introduced into the study of the thiol redox status [26]. Other improved gel-based methods are dependent on the cysteine alkylation reagent-mediated radioactive <sup>14</sup>C-labeling, the fluorescence-labeling and the biotin-HPDP-labeling, which were combined with the two-dimensional differential gel electrophoresis to develop the method of Redox-DIGE [27]. MS-based proteomics is widely used to profile the thiol redox proteome. However, the crucial step of the MS-based proteomics is the enrichment of target peptides. For example, one type of PTM peptides, phosphopeptide, is usually isolated from the total cellular peptide mixture using the immobilized metal-ion affinity chromatography (IMAC) [28], and followed by mass spectrometry analysis to calculate quantitative changes at PTM level [29]. Similarly, to enrich the proteins containing sulfhydryl groups in a MS-based thiol redox study, an thiol affinity chromatography has been developed [30]. Further improvement on this type of method using the biotin-tagged thiol-reactive reagent has made it an acceptable protocol in the thiol redox proteomics [31]. The MS-based thiol redox status measurement methods provide site-specific information in the redox state of cysteines as compared to the gel-based approach. As introduction of the stable isotope labeling into MS-based proteomics study renders it a robust and accurate approach in characterization and quantification of various PTMs in numerous organisms [32-34], it therefore becomes possible to integrate the stable isotope-based chemical labeling into thiol redox proteomics. To do that, a stable isotopic tag is often linked to protein thiol moiety *via* chemical (or enzymatic) reaction during protein sample preparations. A characteristic example of application of this approach in redox proteomics is the stable isotope-coded affinity tag (ICAT)-based redox proteomics [35], in which a <sup>12</sup>C-coded and <sup>13</sup>C-coded 9-carbon linker was introduced and applied to quantify the redox status in two different samples [36,37]. The *OxICAT* [22,38] was developed to differentially label the reduced and the reversibly oxidized cysteine in the single sample for monitoring the cysteine modifications [39]. Alternative to *ICAT* reagent approach, *CysTRAQ* combines *iTRAQ* with a PTM peptide enrichment method to identify and quantify cysteine-containing peptides [40]. This approach was further modified to a tandem chemical labeling approach, in which both *iTRAQ* and the biotinylated thiol-reactive reagents were applied to label the reversibly oxidized cysteine-containing peptides, and named as *OxiTRAQ* [41].

Furthermore, cysteine reactive-tandem mass tag (*CysTMT*) reagents were developed to enable a selective labeling and a relative quantitation of cysteine-containing peptides. This quantification was achieved by measuring a series of reporter ions detected at the lower mass region of

MS/MS spectrum [42]. Recently, the *d0/d5* stable isotope-labeled NEM has also been integrated with the multiple reaction monitoring (*MRM*) mass spectrometry to quantify the site-specific cysteine thiol redox states, and named as *OxMRM* [43]. Another stable isotope labeling strategy is called GEL-based stable isotope labeling of reversibly oxidized cysteine (GELSILOX) method, in which both the control and treated samples was labeled with the stable isotope <sup>16</sup>O and <sup>18</sup>O, respectively, during the process of in-gel digestion of thiol alkylated proteins [44]. Furthermore, the stable isotope metabolic labeling, such as *SILAC*, has gained a wider popularity in quantitative proteomics [45], and has already been applied to study protein thiol modifications in heterotrophic organisms [46,47]. However, the integration of the <sup>15</sup>N stable isotope metabolic labeling with the commonly used chemical labeling-based thiol redox proteomics has not been reported thus far on autotrophic plants. Generally speaking, this strategy integrates the advantages of <sup>15</sup>N stable isotope-labeling in *Arabidopsis* [48] with the robust enrichment of biotin-tagged thiol alkylating reagent-labeling to efficiently purify, accurately identify and quantitatively measure both reduced and reversibly oxidized forms of protein cysteines in a single experiment. This thiol redox proteomics is abbreviated as *OxNSIL* to emphasize its uniqueness to plants. As a result, both reduced and reversibly oxidized forms of protein cysteines are chemically modified with two different alkylating reagents, and each PTM on a cysteine residue can be analyzed quantitatively and independently. Both <sup>14</sup>N/<sup>15</sup>N-coded control and treated *Arabidopsis* cysteine-containing peptides are clearly distinguishable in mass spectrograms and readily used for measurement. It is believed that *OxNSIL* approach can reveal the homeostasis of thiol redox status and quantify the changes of thiol moiety in response to different external or internal cues.

Provided that hydrogen peroxide (H<sub>2</sub>O<sub>2</sub>) increases in plant cells during photosynthesis, photorespiration, and respiration processes [49], and in response to the environmental stresses [50], and that this simplest and uncharged hydrogen peroxide can penetrate membranes through water channel [9], it has been widely used as an oxidative stressor to study the stress responses of plants to ROS attack [23,51]. We hereby present a proof-of-concept study about the application of *OxNSIL* in H<sub>2</sub>O<sub>2</sub>-triggered thiol redox status alteration in *Arabidopsis*. This redox proteomics approach may be useful to the investigation of broader biological problems in other major crops such as rice, wheat, tomato, potato and soybean.

## Materials and Methods

### Plant material, chemical compounds and reagents

The wild type *Arabidopsis thaliana* ecotype *Col-0* (Columbia-0) was obtained from the *Arabidopsis* Biological Resource Center (ABRC, Columbus, OH). Potassium nitrate coded with <sup>15</sup>N stable isotope (99% purity) was purchased from Cambridge Isotopes Laboratories, Ins. (Andover, MA). Trypsin modified by L-1-tosylamido-2-phenylethyl chloromethyl ketone, ACN, TCEP, TFA, Formic acid (FA) and other standard-grade chemicals were purchased from Sigma-Aldrich Co. (St. Louis, MO), whereas EDTA-free protease inhibitor cocktail tablets provided in EASY pack were bought from F. Hoffmann-La Roche Ltd. (Mannheim, Germany). The thiol-specific labeling reagents, 3-(N-Maleimido-propionyl) biocytin (MPB) and N-(biotinoyl)-N<sup>2</sup>-(iodoacetyl)-ethylenediamine (BIAM), were purchased from Invitrogen Co. (Grand Island, NY). Ziptip C<sub>18</sub> was obtained from Millipore (Billerica, MA). Ni-NTA and high capacity streptavidin agarose bead was purchased from Qiagen (Venlo, Netherlands) and

Thermo Fisher Scientific Inc. (Rockford, IL), respectively.

### Plant growth, treatments and isolation of the <sup>15</sup>N/ <sup>14</sup>N-coded total cellular protein

*Arabidopsis* were sown in rows inside glass jars (15 seeds per 9-cm diameter jar) containing SILIA agar medium (either with K<sup>14</sup>NO<sub>3</sub> or K<sup>15</sup>NO<sub>3</sub>) and grown in growth chamber as described previously [48]. Both <sup>14</sup>N- and <sup>15</sup>N-labelled 3-week-old flowering plants were treated in pairs. <sup>15</sup>N-coded plants were subjected to a hydrogen peroxide treatment and the <sup>14</sup>N-labelled plants were used as the control (i.e. Forward labelling) or vice versa (i.e. Reciprocal labelling).

In the H<sub>2</sub>O<sub>2</sub>-elicited oxidative stress treatment, the treated and control plants were completely immersed under 2 mM H<sub>2</sub>O<sub>2</sub> (pH=8.0) aqueous solution and deionized water, respectively, which was followed by vacuum infiltration. The treatment was performed with a pressure of 500 Torr for 10 minutes. Two jars were used for either control or treated group and approximate 1.3 gram tissues were harvested from each jar, and a total of two pairs of *Forward* and *Reciprocal* labeling experimental repeats were performed. Immediately following the treatment, the entire aerial portion of *Arabidopsis* plants was harvested in liquid nitrogen as described previously [52].

In the case of UV-B experiment, two groups of <sup>15</sup>N/<sup>14</sup>N-coded plants were moved into two chambers of 4 white-light lamps (3.07 μE/ m<sup>2</sup>s). UV-B irradiation on the treated group was then provided by 4 additional LZC-UVB photo-reactor lamps (Luzchem Research Inc., Ottawa, ON, Canada), which emit UV-B light with a wavelength peaking at 313 nm. UV-B light irradiation was 0.41 μE/m<sup>2</sup>s in the chamber, which was measured using the IL1700 research radiometer with an UV-B probe (UV Process Supply, Inc. Chicago, IL). Both groups were treated in growth chambers for 15 minutes. Three pairs of forward and reciprocal labeling experiments were performed on both white and UV-B light treated plants.

The <sup>14</sup>N- and <sup>15</sup>N-labeled *Arabidopsis* tissues were ground separately in a -20°C pre-cooled mortar/pestle and then extracted whole cellular proteins using a reductant-free urea-based protein extraction buffer especially designed for *OxNSIL*, containing 150 mM Tris-HCl, pH 7.6, 8 M urea, 0.5% SDS, 1.2% Triton X-100, 20 mM EDTA, 20 mM EGTA, 50 mM NaF, 1 mM PMSF, Complete EDTA free protease inhibitors cocktail, and 2% PVPP modified from the previously reported [48]. The resulting total cellular proteins were dissolved in a cold reductant free re-suspended buffer (RSB) containing 8 M urea, 300 mM NaCl, 0.5% Nonidet P-40, and 50 mM Tris, pH 8.0. The concentration of protein was measured by a protein DC assay (Bio-Rad Laboratories, Inc. Hercules, CA) and calculated according to a bovine serum albumin (BSA) protein standard curve. Approximately 12 mg of the total cellular proteins were extracted from 1 gram of tissue. The isolated protein samples were stored at -80°C for later use.

### In vitro conjugation of peptide with thiol-specific biotinylating reagents

The widely used thiol alkylation reagents, MPB and BIAM [23,53-56], were dissolved in solvent dimethyl sulfoxide to make a stock solution. The synthetic peptides P1 (HHHHHHPLKKKLDEFGSRLTTAIC) and P2 (HHHHHHRSYLCGDEFNSVRAVND), derived from calcium-transporting ATPase (AT4G00900) and calmodulin binding IQ-domain 33 (AT5G35670), respectively, was dissolved in RSB solution and mixed with MPB and BIAM, respectively. After the reaction, peptides, P1 and P2, were enriched using Ni-NTA agarose beads and subjected to on-beads trypsin digestion as previously described

[52]. The digested peptides were desalted using C<sub>18</sub> Ziptip (Millipore, Billerica, MA) for the subsequent MS analysis.

To label the reduced form of cysteines, the mixture of <sup>14</sup>N- and <sup>15</sup>N-coded total cellular proteins in RSB solution was supplemented with MPB to a final concentration of 1 mM and incubated for 2 hours with constant rotation at room temperature. Afterwards, cysteine was added to the mixture with a final concentration of 10 mM to titrate out the excess amount of MPB [23]. Following the incubation at room temperature for another hour, the mixed total proteins were precipitated by cold mixture of acetone and methanol (12:1 in v/v) and re-suspended in RSB solution again. To distinctively label the reversibly oxidized form of thiol group of cysteine, TCEP was added to the protein sample with a final concentration of 5 mM and incubated at room temperature for an hour to reduce the reversibly oxidized form of cysteines to free thiol groups [57]. BIAM was added thereafter to a final concentration of 1 mM for the alkylating reaction to proceed for another 4 hours at room temperature. Finally, the dual chemically labeled protein samples were precipitated and stored at -80°C for later SDS-PAGE fractionation.

### SDS-PAGE fractionation of thiol-reactive compound-tagged proteins and in-gel trypsin digestion

A total of 10 mg of thiol alkylated protein mixture (<sup>15</sup>N/ <sup>14</sup>N) was loaded onto one 190 mm×180 mm preparative SDS-PAGE slab gel (10%). A small fraction of slab gel was sliced vertically and stained with Coomassie brilliant blue to examine the quality of electrophoresis separation of sample proteins. The rest part was sliced horizontally and evenly into 10 strips and further diced into 1-mm<sup>3</sup> cubes. The in-gel trypsin digestion was performed as previously described [52]. The digested peptides were extracted from the gel cubes by 1% FA in 50% ACN for 3 times. The ACN solvent in the combined peptide extract in each falcon tube was vaporized, lyophilized to a complete dry powder and then stored at -80°C.

In the case of Western blot analysis, the total cellular proteins extracted from both <sup>14</sup>N- and <sup>15</sup>N-coded *Arabidopsis* plants were either directly fractionated on SDS-PAGE or alkylated first with one of the reagents, BIAM or MPB, and followed by SDS-PAGE fractionation. Finally these labeled and unlabeled proteins were transferred onto PVDF membrane from SDS-PAGE and hybridized with anti-biotin (Sigma A4541) antibodies.

### Streptavidin affinity enrichment of biotinylated peptides

The dried peptides were dissolved in falcon tubes by 1 mL binding buffer (50 mM Tris-HCl, 100 mM NaCl, pH 8.0). Afterwards, 0.1 mL of streptavidin beads (Thermo Fisher Scientific Inc., Rockford, IL USA) slurry pre-equilibrated by the binding buffer was added into the peptide solution, and the affinity binding was allowed to proceed at room temperature for an hour. After beads were washed twice with the binding buffer containing 0.2% SDS and further washed with deionized water twice, elution buffer consisting of 70% FA and 30% ACN [58] was added to beads and incubated at 70°C for 5 min. The supernatant was collected and evaporated inside of a speed vac. Eluate was dissolved in 0.1% TFA and desalted on C<sub>18</sub> Ziptip for MS analysis.

### LC-MS/MS data acquisition and analysis

Mass spectrometry analysis of biotinylated peptides was performed using a nano-flow Liquid chromatography (nanoLC Acquity™, Waters, Milford, MA) coupled to an ESI-hybrid Q-TOF tandem mass spectrometer (Premier, Waters). A 180 μm × 20 mm Symmetry C<sub>18</sub> trap

column and 75  $\mu\text{m} \times 250$  mm BEH130  $\text{C}_{18}$  analytical column were used on nanoUPLC. The mass spectrometer is operated in a positive ion mode with the following basic parameters: source temperature 80°C, capillary voltage 2.4 KV and sample cone voltage 35 V. The collision energy was variable during MS/MS scan according to  $z$  and  $m/z$ . The exact setting values followed the instruction of MS machine manufacturer. Mass spectra of peptides were acquired using data-dependent acquisition mode. The data-dependent analysis was set as the following: 1 s MS and to maximum 3 s MS/MS,  $m/z$  50-2500 (continuum mode) and 60 s dynamic exclusion. The +2, +3 or +4 charged ions, whose intensity rose above 40 counts/second, were subjected to the consequent MS/MS scan survey. MassLynx (version 4.1, Waters) was used for data acquisition and instrument control.

### Identification of thiol-reactive compound-tagged $^{15}\text{N}/^{14}\text{N}$ -coded peptides

Tandem mass spectrometry raw data were processed using ProteinLynx (version 2.2.5, Waters) first to generate a list of MS/MS files and related retention time. The resulting MS dataset was searched against TAIR10 protein database (The *Arabidopsis* Information Resource 10, <http://www.Arabidopsis.org/>) [59] using commercially available Mascot Server (Version 2.3, Matrix Science, London, UK). The searching parameters were set as such that up to one missed cleavage site is allowed. Mass tolerances were  $\pm 50$  ppm for MS precursor ions and 0.2 Da for MS/MS fragment ions, respectively. A built-in Mascot quantitation method, named " $^{15}\text{N}$  metabolic", was used to identify  $^{15}\text{N}$ -coded and thiol-reactive compound-modified peptides. Biotin(K), Oxidation(M) and three custom-defined modifications, *i.e.* MPB(C), MPB[H](C) and BIAM(C), which stands for MPB, hydrolyzed MPB and BIAM tagged on cysteines, respectively, were set as the variable PTM. The hydrolyzed MPB was introduced because that the product of MPB with cysteine, succinimidyl thioether, is easily hydrolyzed during the following multiple steps [60,61]. Since the nitrogen element in both MPB and BIAM molecules are all  $^{14}\text{N}$  regardless of whether the alkylated peptides are either  $^{15}\text{N}$ - or  $^{14}\text{N}$ -coded peptides and Mascot search engine cannot distinguish between atoms in amino acid residues and that in modification group, the formulas set for the modifications (*i.e.*  $\text{C}_{23}\text{H}_{33}\text{N}_5\text{O}_7\text{S}$ ,  $\text{C}_{23}\text{H}_{35}\text{N}_5\text{O}_8\text{S}$  and  $\text{C}_{14}\text{H}_{22}\text{N}_4\text{O}_3\text{S}$  for MPB(C), MPB[H](C) and BIAM(C), respectively) were modified to the ones having approximately equal mono- isotopic mass (difference  $< 0.03$  Da) but without nitrogen atom in Mascot search (*i.e.*  $\text{C}_{15}\text{H}_{39}\text{O}_{19}\text{S}$ ,  $\text{C}_{15}\text{H}_{41}\text{O}_2\text{S}$  and  $\text{C}_{16}\text{H}_{22}\text{O}_5\text{S}$  for MPB(C), MPB[H](C) and BIAM(C), respectively). Expectation value ( $E$ -value) was defined as a composite score of peptide identification to calculate false discovery rate (FDR) based on separated target-decoy search. Then identifications were filtered to  $\text{FDR} \leq 1\%$ .

### Quantitative analysis of $^{15}\text{N}/^{14}\text{N}$ -coded peptides

The paired  $^{15}\text{N}/^{14}\text{N}$  ion intensities of each peptide were calculated as described [48,62]. Ion chromatograms of the monoisotopics of both  $^{14}\text{N}$  and  $^{15}\text{N}$  isotopic envelopes were calculated by integrating areas under the chromatographic peaks, in which the peptide MS/MS survey was performed. The isotopologue distributions of both  $^{14}\text{N}$ - and  $^{15}\text{N}$ -coded peptides were obtained based on the Yergey algorithm [63]. When calculating the isotopologue distribution of heavy nitrogen-coded peptides, a 97.43% incorporation rate of  $^{15}\text{N}$  into light nitrogen-coded peptides was measured following a procedure described previously [48]. The ion counts of the whole isotopic envelopes of both  $^{14}\text{N}$ - and  $^{15}\text{N}$ -coded peptides were calculated using ion counts from the monoisotopic peak over its isotopologue distribution [48,62]. To estimate actual ratio of  $^{15}\text{N}/^{14}\text{N}$ -coded total proteins at the initial

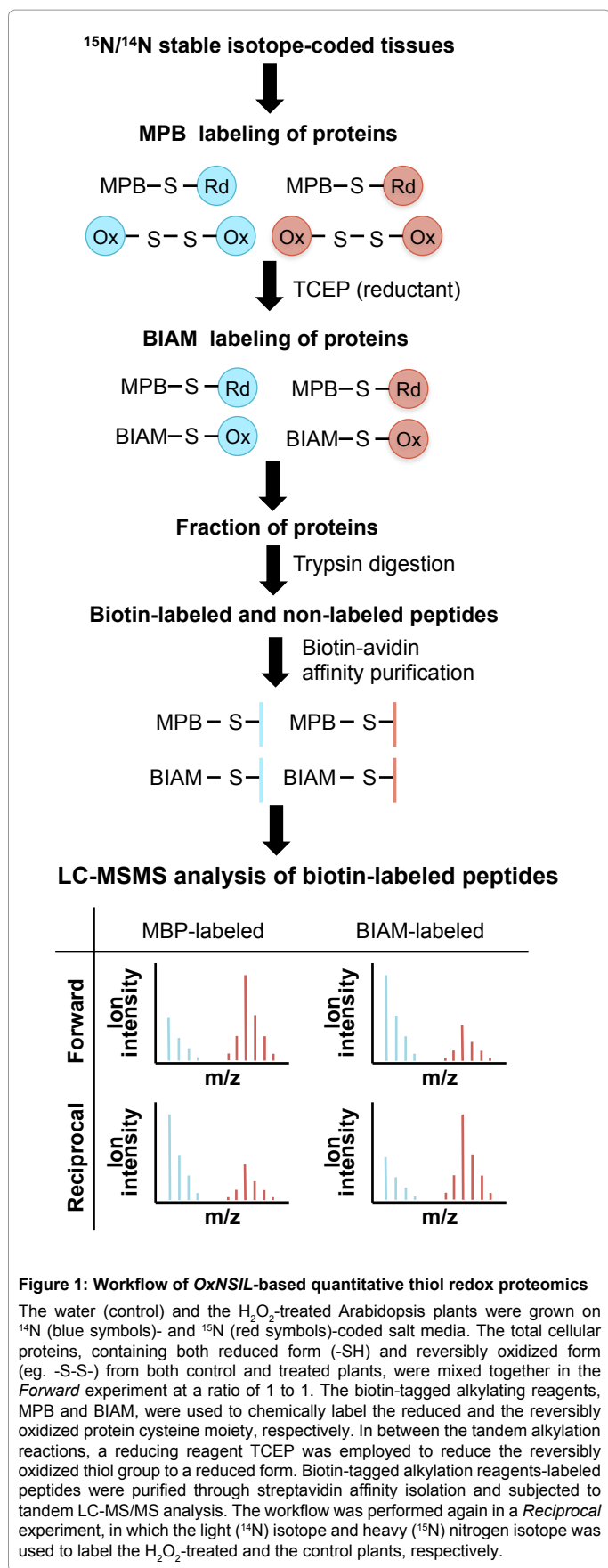
mixing, the ratios of 4 representative peptides lacking of cysteine derived from one of the most abundant protein, the large subunit of RuBisCO (ATCG00490), were calculated. The average ratio of these 4 peptides in each biological replicate (both *forward* and *reciprocal*) was used as the negative control to calibrate the ratios of all  $^{15}\text{N}/^{14}\text{N}$ -coded peptides following the previous algorithm [62]. Finally, the statistical significance was obtained by applying a two-tailed t-test (unequal variance) followed by multiple hypothesis testing correction using Benjamini-Hochberg method ( $\text{FDR} \leq 5\%$ ) [64]. More stringently, those BIAM- to MPB-labeled peptide isoforms whose  $\log_2$  changes locate in the range of  $[-0.15, 0.15]$  ( $\sim 10\%$ ) were eventually filtered out, considering the intrinsic noise of mass spectrometry measurement and possible errors during experiment [48].

## Results and Discussion

### OxNSIL

The heavy nitrogen stable isotope labeling-based quantitative proteomics (SILIA) has been successfully applied in the quantitation of phosphopeptides from both hormonal mutants and hormone-treated *Arabidopsis* [62]. In the present study, we intend to integrate the stable isotope metabolic labeling of entire plants with the dual chemical labeling method using biotin-tagged alkylation reagents to differentially measure both reduced and oxidized thiols. The workflow of OxNSIL is shown in Figure 1. Firstly, both the control and the treated plants were grown either on a medium containing the natural abundance of nitrogen isotope ( $^{14}\text{N}$ -coded salt) or a medium containing the heavy nitrogen isotope ( $^{15}\text{N}$ - coded salt). The harvested plant frozen tissue powders were extracted using a protein-denaturing buffer to isolate total cellular proteins. Although acidification is the common practice to freeze the redox states, it may perturb thiol-disulfide equilibria because the biological thiols have a wide range of the acidity ( $pK_a$ ) values [65]. To maintain the native redox status of thiol groups before chemical labeling, the enzyme- catalyzed thiol-disulfide exchange in this OxNSIL approach was abolished because the protein catalysts are inactivated under denature condition, whereas the non-enzymatic reaction of thiol-disulfide exchange is believed to be slow due to the low nucleophilicity of the thiol reactant at physiological pH [66]. The differentially isotope-coded control and treated proteins were mixed at an equal amount (1:1) in order to alkylate the cysteinyl proteins from both control and treated samples in parallel. Considering the cysteine alkylation and other experimental variation in different samples and negligible redox exchange under our experimental condition, we mixed the control and treated sample together to perform the following steps side by side. Afterwards, the protein mixture was firstly labeled with thiol-reactive reagent MPB ( $\text{C}_{23}\text{H}_{33}\text{N}_5\text{O}_7\text{S}$ , molecular weight=523.6 Da), followed by a reductant TCEP, and finally treated with a second thiol-reactive reagent BIAM ( $\text{C}_{14}\text{H}_{23}\text{IN}_4\text{O}_3\text{S}$ , molecular weight=454.3 Da) in a sequential order.

These multiple steps of chemical reactions were designed to label free thiols of protein with MPB, followed by a reduction of the reversibly oxidized thiols, and finally to label the TCEP-converted free thiols of protein (equivalent to reversibly oxidized thiols) with BIAM (Figure 1). The biotin-tagged alkylating reagents have been widely used as thiol-reactive reagents since it provides an advantage in the affinity purification for cysteine containing peptides [41]. These redox PTM proteins were then digested by trypsin and enriched by streptavidin beads. Finally, the enriched cysteine-containing peptides were analyzed by LC-MS/MS (Figure 1). As a result, the difference in thiol redox status between the control and the treated plants in the



*Forward* and *Reciprocal* experiment can be quantified based on MS data (Figure 1). As compared to the 2DE-based thiol redox proteomics, OxNSIL approach, similar to the methods of ICAT, OxICAT, CysTMT, CysTRAQ, OxMRM, and OxITRAQ, focuses on the site-specific, comprehensive and quantitative study of oxidative and/or reductive alteration of any cysteine-containing proteins in any plants that can be metabolically labeled with stable isotope. One of advantages of OxNSIL over the OxICAT, OxITRAQ and OxMRM is that it may offer a relatively economic way to analyze plant redox-sensitive proteins in a site-specific fashion and at a large scale because 10 mg of the starting <sup>15</sup>N- coded total cellular protein require about a gram of <sup>15</sup>N-coded plant tissue [48] that costs USD 9 to 42 to grow (depending on the developmental stages and light conditions).

A pair of *Forward* (i.e. both <sup>14</sup>N-labeled control plant protein and <sup>15</sup>N-labeled and treated plant protein are mixed) and *Reciprocal* (i.e. both <sup>15</sup>N-labeled control protein and <sup>14</sup>N-labeled and treated plant protein are mixed) were performed to eliminate any isotope effects resulting from heavy nitrogen labeling during measurement and this pair of experiment was repeated once to meet the requirement for redox PTM peptide quantitation. To validate the reaction of these biotin-tagged alkylation reagents with cysteine-containing peptides, both polyhistidine-tagged peptides HHHHHHPLKKKLDEFGSRLTTAIC and HHHHHHRSYLCGDEFNSVRAVND, of which cysteine locates either at the C-terminal end or in the middle of peptides, were synthesized chemically and reacted with both MPB and BIAM. The mass shift of 523.21 Da for MPB labeling and 326.14 Da for BIAM labeling were found from MS/MS spectra (Figures 2A to 2D), which reflect exactly the additional mass of the modifications on the peptides resulting from the reactions with MPB and BIAM by free thiols of cysteine residues (Figures 2E and 2F).

The biotin-tagged alkylation of total cellular protein was further validated with anti-biotin immuno-blotting analysis (Figure 2G). As compared to the two bands shown in the Western-blot of non-alkylated total protein sample, numerous bands were detected from the BIAM-labeled total cellular proteins, suggesting a successful conjugation of BIAM to cysteine thiol in both <sup>14</sup>N and <sup>15</sup>N-labeled proteins. According to the same results, we can conclude that the thiol alkylation does not have bias toward either light or heavy nitrogen isotope-coded cellular proteins, which had been further confirmed from MS results (Figure 2H). To assess if biotin-tagged alkylation affects the accuracy of OxNSIL-based protein measurement, the standard conversion curves from the peptide ion intensity to protein were established for both non-cysteine-containing and MPB-labeled peptides. The log<sub>2</sub> ratios (x) of whole isotopic envelopes of <sup>15</sup>N/<sup>14</sup>N-labeled peptides are correlated to the log<sub>2</sub> ratios of the initially mixed <sup>15</sup>N/<sup>14</sup>N-labeled total cellular proteins (y). The equation of y=1.13x - 0.19 and y=1.15x - 0.42 was obtained for the non-cysteine containing and the alkylating reagents-labeled protein samples, respectively (Supplementary Figure 1). Due to the limitation of dynamic range in mass spectrometry, incomplete <sup>15</sup>N incorporation and the existence of periodic noises, the ratio of <sup>15</sup>N-/<sup>14</sup>N-coded peptides calculated from MS spectrum is not exactly the same as the ratio, by which two sample proteins were mixed. A standard curve is normally used to convert the observed ratio of twin isotopic envelopes into the real ratio of the differentially labeled PTM protein isoforms. According to the results, there is no significant difference between the two standard conversion curves in the measurement of the non-cysteine containing and the thiol-alkylated peptides, which suggests that biotin-tagged thiol alkylation does not influence the ratio of peptide ion intensity measurement (Supplementary Figure 1).

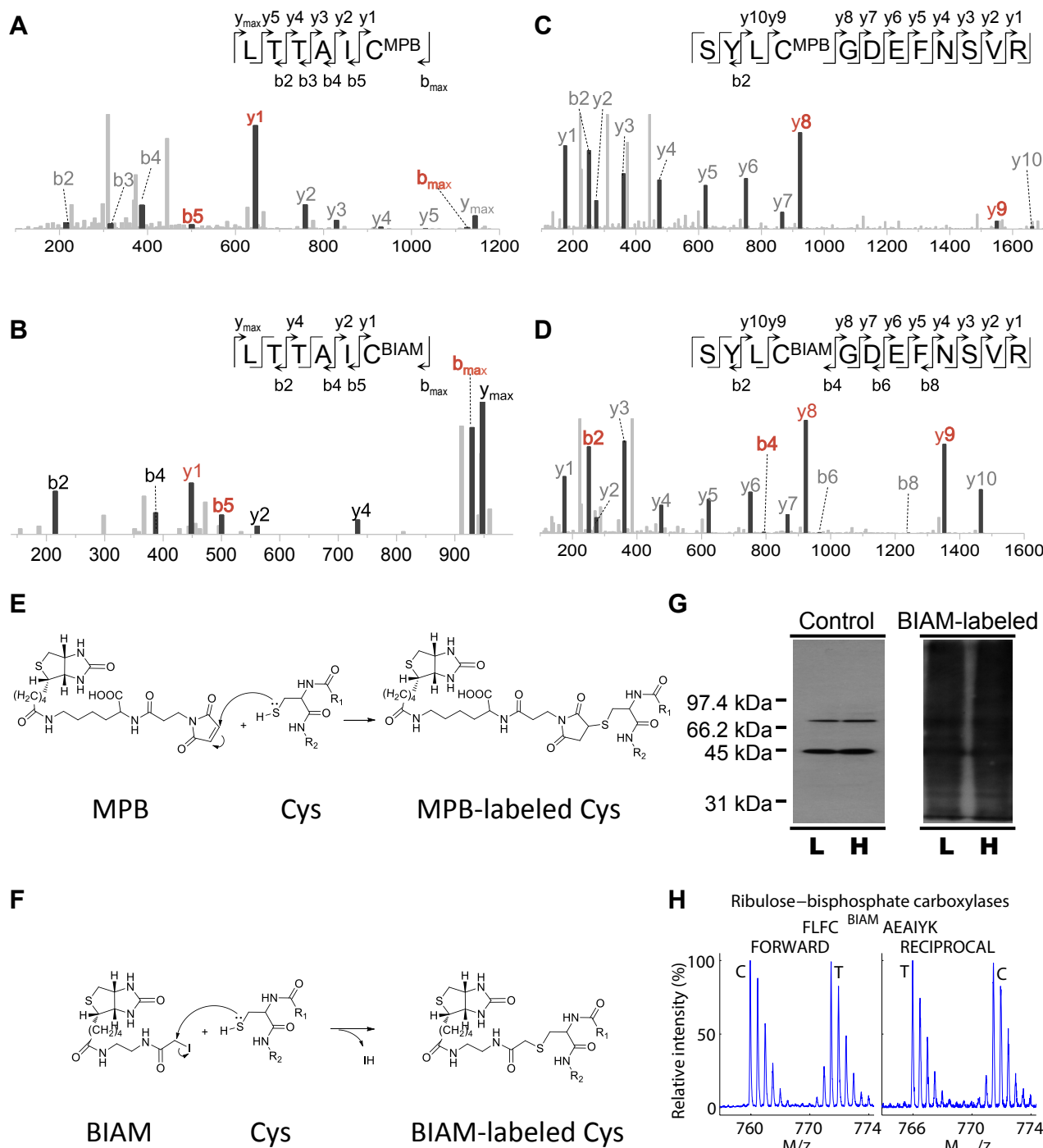


**Figure 2: Biotin tagged Cysteine alkylation and mass spectrometry-based quantitation of cysteine-containing peptide and protein**

(A) to (D) is the MS/MS spectrum of MPB/BIAM-labeled two synthetic peptides ion precursors (charge 2). The ratio of mass to charge ( $m/z$ ) is 527.7726 (A), 474.2459 (B), 956.8995 (C), and 858.3426 (D), respectively, corresponding to oligopeptide LTTAIC from calcium-transporting ATPase (AT4G00900) and oligopeptide SYLCGDEFNSVR from calmodulin binding IQ-domain 33 protein (AT5G35670). The site-specific labeling occurs at the C-terminus of LTTAIC and the middle of SYLCGDEFNSVR, respectively.

(E) and (F) illustrates the chemical reaction of MPB and BIAM with the thiol moiety of cysteine residue, respectively.

(G) is the anti-biotin immune-blotting analysis of the biotin-tagged alkylation of the total cellular protein, which was isolated from  $^{14}N$  - (L) and  $^{15}N$ -coded (H) wild type plant, respectively.

(H) illustrates an MS<sup>1</sup> spectrum example of biotin-tagged alkylating reagents labeled peptide from mixed  $^{14}N$  - and  $^{15}N$ -labeled plant samples. The differentially stable isotope-labeled total proteins were mixed at a ratio of 1:1. Forward and Reciprocal refers to the order of mixing  $^{14}N$ -coded control (C) protein with  $^{15}N$ - coded treated (T) protein and vice versa, respectively. Superscript BIAM marks the cysteine residues labeled by BIAM. M/z represents the ratio of the ion mass to the charge of each PTM peptide.

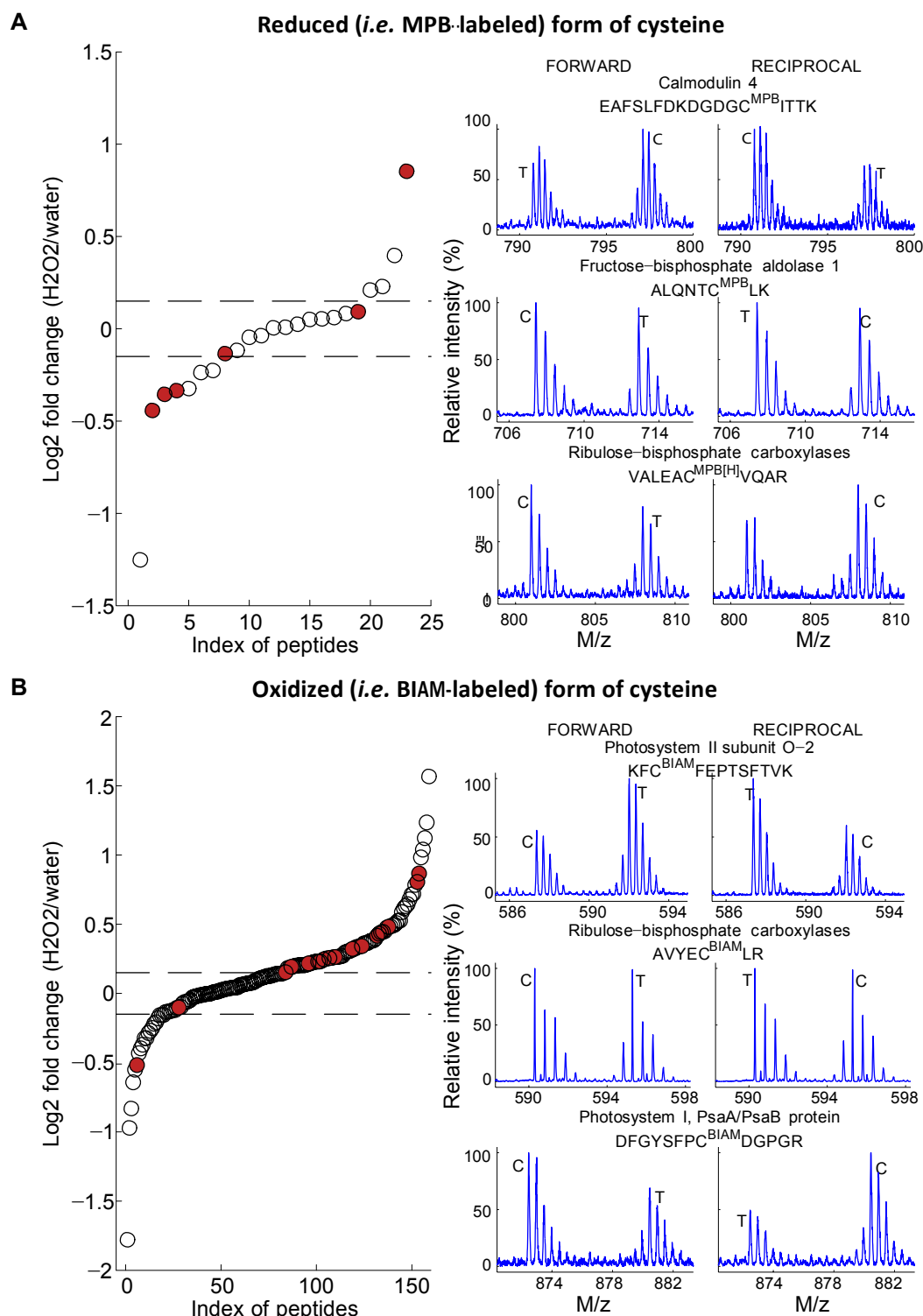


**Figure 3: OxNSIL-based quantitative and differential thiol redox proteomic analysis of alkylating reagent-labeled PTM peptides.**

(A) and (B) represents the alteration in the reduced form (MBP-labeled or hydrolyzed MPB-labeled) and the oxidized form (BIAM-labeled) of peptides identified from H<sub>2</sub>O<sub>2</sub>-treated samples, respectively. The MS<sup>1</sup> spectrum examples of decreased, unchanged and increased ratio of peptides between the treated and control sample are shown on the right panels in each set. Each circle (open and solid) represents the average ratio of the peptide amount of a certain labeled PTM peptide identified from both the treated and control. Those PTM peptides of statistical significance given by student's *t*-test are marked as darker solid circle. The dash lines delineate the cutoffs ( $\pm 0.15$ ) of significant alteration (see Experimental Procedures).

Forward and Reciprocal refers to the order of mixing <sup>14</sup>N-coded control (C) protein with <sup>15</sup>N-coded treated (T) protein and vice versa, respectively. Superscript MPB, MPB[H] and BIAM marks the cysteine residues labeled by MPB, hydrolyzed MPB and BIAM, respectively. M/z represents the ratio of the ion mass to the charge of each PTM peptide.

### MS-based profiling of thiol-alkylated PTM peptides from H<sub>2</sub>O<sub>2</sub>-treated *Arabidopsis*

Once the OxNSIL protocol was established, it was applied in the study of the thiol redox state alteration in *Arabidopsis* triggered by H<sub>2</sub>O<sub>2</sub> treatment. In order to identify ROS-modified cysteines, a large scale of BIAM and MPB alkylation-based profiling of the total cellular protein of stress-treated *Arabidopsis* was performed according to the workflow shown in Figure 1. The resulting peptide samples were analyzed by nano-LC-ESI-Q-TOF mass spectrometry (See Materials and methods for details). A total of 52,475 spectrum-peptide matches were given by Mascot search engine, which include both non-alkylated and MPB/BIAM-alkylated peptides. The *E*-value was defined as a composite score for the quality assessment of identification and the peptide spectra-matching results were filtered according to FDR ≤ 1%. Threshold of *E*-value for single isotope-coded peptide identification was determined to be 0.11 to meet such a FDR.

Moreover, the identification was also selected if they appeared in pair since the maximum FDR for the peptides identified in pair is less than 0.8%, indicating that paired identification offers a strong evidence for true positive results. Filtered using these two criteria, 10,739 peptides were obtained, among which 1,412 and 9,220 are MPB- and BIAM-labeled cysteine-containing peptides, respectively, and only 107 are non-labeled peptides. To further validate the efficiency of biotin-tag enrichment, a strip from SDS-page gel was randomly selected from each biological replicate and went through the following steps without affinity enrichment. As a result, 1,674 peptides were obtained, out of which only 46 of them are thiol-alkylated peptides. Taken together, 36 folds enrichment (i.e. from 2.75% to 99%) was achieved through OxNSIL approach. Eventually, obtained were 438 non-redundant biotin-tagged thiol-alkylated peptides representing 391 different cysteine-containing proteins of non-redundant Genebank accession numbers, implying that more than one thiol-alkylated peptides were identified from a single protein. The sharp reduction in non-redundant peptide number (10,739 peptides to 438 non-redundant peptides) as compared to that of the initial MS measurement is due to fact that RuBisCO protein accounts up to 65% of the soluble protein in adult plants [67] and have been confirmed in a number of proteomics studies [68]. It is a general problem specific for plant proteomics because some peptides are frequently detected for hundreds of times, such as the peptides derived from RuBisCO proteins, if the specific RuBisCO removal strategies are not applied during protein isolation [69,70]. To perform differential thiol redox proteomic analysis, 285 repetitively (at least twice) detected peptides were selected from those 438 non-redundant thiol-alkylated peptides (Supplementary Table 1). Among these biotin-tagged peptides, 216 BIAM- labeled and 28 MPB-labeled peptides were identified from 4 groups of the control water-treated plants whereas 230 BIAM-labeled and 33 MPB-labeled peptides from 4 groups of 2 mM hydrogen peroxide- treated plants, suggesting that OxNSIL protocol is able to enrich and identify both thiol-reduced and - oxidized PTM peptides (Figure 4).

### OxNSIL-based quantitative measurement of H<sub>2</sub>O<sub>2</sub>-modified redox proteins

As a relatively moderate and naturally occurring ROS in plant cell, H<sub>2</sub>O<sub>2</sub> has been widely applied in redox study [23,39]. To elucidate ROS-sensitive protein thiol sites, OxNSIL was applied onto hydrogen peroxide-treated *Arabidopsis* to investigate the change of cysteine redox status caused by 2 mM H<sub>2</sub>O<sub>2</sub> at 10 minutes of induction. Out of 285 repetitively detected thiol-alkylated peptides (Supplementary

Table 1), 23 MPB- and 159 BIAM-labeled peptides were selected out for quantitative thiol redox proteomic analysis (Supplementary Tables 2 and 3). The criteria for selecting these measurable peptides were: 1) they were detected for at least 3 times, 2) they were detected in both *Forward* and *Reciprocal* experiments, and 3) they were found in both <sup>14</sup>N- and <sup>15</sup>N-coded peptide ion isoforms. Lastly, the light and heavy MPB-/BIAM-labeled peptide isotope envelopes were measured only after the MS spectrum of each peptide was verified by the manual spectrum inspection and all MS spectra of overlapping noise ion(s) had been removed.

Because light and heavy isoforms of a peptide produce distinct isotope envelopes, the ratio of twin isotopic envelopes of each peptide were calculated based on the extracted ion chromatograms of monoisotopic peaks and its isotopic distribution (see Materials and methods). Both two-tailed *t* test and Benjamini-Hochberg multiple hypothesis testing correction (FDR ≤ 5%) [64] were performed on the measurement of peptide to determine the statistical significance. Considering the intrinsic noise of mass spectrometry measurement and possible errors during experiment [48], those peptides whose log<sub>2</sub> changes locate in the range of [-0.15, 0.15] were further filtered out (Figure 3). As a result, 1 reduced (MPB-labeled) and 16 oxidized (BIAM-labeled) isoforms of peptides that were significantly down- and up-regulated by 10-min H<sub>2</sub>O<sub>2</sub> treatment, respectively, were found and listed in Table 1 (and Supplementary Figure 2). Since some peptides are conserved among a protein family, these 17 peptide isoforms represent 27 proteins whose cysteine residues were oxidized by H<sub>2</sub>O<sub>2</sub> (Table 1).

Consistent with the previously reported from H<sub>2</sub>O<sub>2</sub>-treated plant cells, proteins observed in Table 1 were oxidized by H<sub>2</sub>O<sub>2</sub> and the oxidation of cysteine residues was mainly found on the proteins that function in Calvin cycle (8 peptides) and translation-related processes (4 peptides), whereas other oxidized proteins belong to ferredoxin/thioredoxin system, photosynthesis and lipid transport. These results are comparable to the previous discovery that these cellular events are very sensitive to redox changes and that alterations of redox status of many proteins are related to these two processes and they have been repetitively reported in previous redox studies [71]. It has been reported that the 427th cysteine residue (C427) of RBCL and C175 of RuBisCO activase (RCA, AT2G39730) were S-nitrosylated in the *Arabidopsis* suspension cells grown in liquid Murashige and Skoog (MS) medium [72] while Phosphoribulokinase (PRK, AT1G32060) can also be S-nitrosylated [73]. In addition, it has been demonstrated in *Chlamydomonas reinhardtii* that the thiol moieties of RBCL are oxidized in the oxidative environment, through which the activity of RuBisCO is regulated [74,75] and the activity of its PRK is regulated through forming and breaking of disulfide bridge [76]. Moreover, the aldolase proteins can form disulfide bond with glutathione when incubated with GSSG [77] and the conserved C197 of Fructose-bisphosphate aldolase 6/8 (FBA6/8, AT2G36460/ AT3G52930), locating within the enzyme active site [78], alters its disulfide bond in response to cellular redox status. Oxidation of C44 and C47 (i.e. C96 and C99 of precursor protein) of Ferredoxin 1/2 (FD1/2, AT1G10960/AT1G60950), two of the 4 cysteinyl ligands coordinating with 2Fe-2S cluster, were also observed under H<sub>2</sub>O<sub>2</sub>-treatment. The assembly of the cluster may be disrupted by the attack of external ROS, which leads to a reduction in ferredoxin/thioredoxin system, and causes it to lose its reductive power in the H<sub>2</sub>O<sub>2</sub>-treated plants. Furthermore, it was reported that C81 of *E. coli* GTPase elongation factor, which is homologous to C137 of the GTP binding Elongation factor Tu family protein (AT4G02930) in *Arabidopsis* (two proteins share 70% homology), plays a critical functional role in aminoacyl-tRNA binding [79]. Taken together,

Accession No.	Log2 ratio	p-value <sup>a</sup>	Peptide <sup>b</sup>	Protein
<b>Decrease of reduced form (-SH) alkylated with MPB</b>				
CALVIN CYCLE				
ATCG00490	-0.33	5.0 × 10 <sup>-11</sup>	<sup>422</sup> VALEAC <sup>MPB</sup> VQAR	Ribulose biphosphate carboxylase large chain (RBCL)
<b>Increase of oxidized form (-S-S-) alkylated with BIAM</b>				
CALVIN CYCLE				
AT1G67090,	0.43	2.9 × 10 <sup>-2</sup>	<sup>91,91,91,91</sup> NKWIPC <sup>BIAM</sup> VEFELEHGFVYR	RuBisCO small subunit
AT5G38430,	0.26	9.2 × 10 <sup>-5</sup>	<sup>141,141,141,141</sup> EVEEC <sup>BIAM</sup> KK	1A/1B/2B/3B
AT5G38420,	0.16	4.4 × 10 <sup>-4</sup>	<sup>127,127,127,127</sup> LPLFGC <sup>BIAM</sup> TDSAQVLK	(RBCS1A/1B/2B/3B)
AT5G38410				
AT2G36460, AT3G52930	0.42	7.3 × 10 <sup>-4</sup>	<sup>197,197</sup> C <sup>BIAM</sup> AAVTER	Fructose-bisphosphate aldolase 6/8 (FBA6/8)
AT1G32060	0.26	1.4 × 10 <sup>-3</sup>	<sup>292</sup> KLTC <sup>BIAM</sup> SYPGIK	Phosphoribulokinase (PRK)
AT2G39730	0.22	1.4 × 10 <sup>-6</sup>	<sup>172</sup> SFQC <sup>BIAM</sup> ELVMAK	RuBisCO activase (RCA)
AT2G21170	0.20	3.1 × 10 <sup>-2</sup>	<sup>199</sup> TFDVC <sup>BIAM</sup> FAQLK	Triosephosphate isomerase (TIM)
TRANSLATION-RELATED PROTEINS				
AT1G14320, AT1G26910, AT1G66580	0.87	4.8 × 10 <sup>-2</sup>	<sup>122,122,122</sup> ALGTC <sup>BIAM</sup> AR	Ribosomal protein L10 A/B/C (RPL10A/B/C)
AT3G48930; AT4G30800; AT5G23740	0.48	3.8 × 10 <sup>-2</sup>	<sup>59,59,59</sup> C <sup>BIAM</sup> PFTGTVSIR	Embryo defective 1080 (EMB1080); Nucleic acid-binding, OB-foldlike protein; Ribosomal protein S11-beta (RPS11-BETA)
AT4G20360; AT4G02930	0.45	2.1 × 10 <sup>-3</sup>	<sup>143,131</sup> HYAHVDC <sup>BIAM</sup> PGHADVVK	RAB GTPase homolog E1B (RABE1b); GTP binding Elongation factor Tu family protein
AT3G11940, AT2G37270	0.23	4.6 × 10 <sup>-2</sup>	<sup>67,67</sup> AQC <sup>BIAM</sup> PIVER	Ribosomal protein 5A/B (RPS5A/B)
PHOTOSYNTHESIS				
AT5G66570, AT3G50820	0.34	1.5 × 10 <sup>-3</sup>	<sup>135,134</sup> KFC <sup>BIAM</sup> FEPTSFTVK	Photosystem II subunit O-1/2 (PSBO1/2)
AT4G02770, AT1G03130	0.32	1.6 × 10 <sup>-5</sup>	<sup>132,128</sup> KEQC <sup>BIAM</sup> LALGTR	Photosystem I subunit D-1/2 (PSAD-1/2)
LIPID TRANSPORT				
AT2G10940	0.25	2.7 × 10 <sup>-4</sup>	<sup>215</sup> LGAC <sup>BIAM</sup> VDLLGGLVK	Bifunctional inhibitor/lipidtransfer protein/seed storage 2S albumin superfamily protein
	0.23	4.2 × 10 <sup>-2</sup>	<sup>206</sup> ATC <sup>BIAM</sup> PIDTLK	
FERREDOXIN/THIOREDOXIN SYSTEM				
AT1G10960, AT1G60950	0.44	4.4 × 10 <sup>-8</sup>	<sup>93,93</sup> AGSC <sup>BIAM</sup> SSC <sup>BIAM</sup> AGK	Ferredoxin 1/2 (FD1/2)

<sup>a</sup>Given by two-tailed Student's *t*-test. All peptides listed were selected using two-tailed Student's *t*-test with Benjamini-Hochberg multiple hypothesis testing correction (FDR ≤ 5 %).

<sup>b</sup>The cysteines (C) labeled by MPB and BIAM are marked by superscript <sup>MPB</sup> and <sup>BIAM</sup>, respectively.

**Table 1:** Oxidation of cysteine residues induced by 10-minute H<sub>2</sub>O<sub>2</sub> treatment.

previous reports [80] support our thiol redox proteomic findings from 10 min H<sub>2</sub>O<sub>2</sub>-treated plants and dismiss the possibility that the mild stress treatment may be lethal to plants.

Interestingly, besides the 17 peptides shown in Table 1, 3 more peptides were oxidized by 10-min H<sub>2</sub>O<sub>2</sub> treatment (*i.e.* increase in oxidized isoforms or decrease in reduced isoforms) whereas 2 peptides were found to be reduced by the treatment (*i.e.* decrease in oxidized isoforms or increase in reduced isoforms) (Supplementary Tables 4 and 5) if only a two-tailed *t* test (*p*<0.05) was used. These two cysteine residues that were reduced after the treatment, C27 of Calmodulin 1/2/3/4/5/6/7 (CaM1/2/3/4/5/6/7, AT5G37780/ AT2G41110/ AT3G56800/ AT1G66410/ AT2G27030/ AT5G21274/ AT3G43810) and C559 of PsaA/PsaB proteins (PSAA/B, ATCG00350/

ATCG00340), subunits of photosystem I reaction center are both novel ROS-regulated thiol sites. The reduced forms of calmodulin 1/2/3/4/5/6/7 and the oxidized forms of PsaA/PsaB protein increased and decreased upon H<sub>2</sub>O<sub>2</sub> treatment, respectively. It has been reported that both C27 of CaM and C559 of PSAB could be S-nitrosylated [72,81]. Interestingly, the C27 site of CaM1/2/3/4/5/6/7 is a unique and highly conserved cysteine residue among plant calmodulins. Given that CaM is the primary intracellular calcium sensor that regulates numerous protein functions in various cellular processes [82] and is strongly conserved across all eukaryotes [83], the increase of reduced form of calmodulin upon rapid H<sub>2</sub>O<sub>2</sub>-induction suggests that these calcium-binding proteins may function to be crosstalk between thiol redox regulation and calcium signaling. Especially interesting is that as

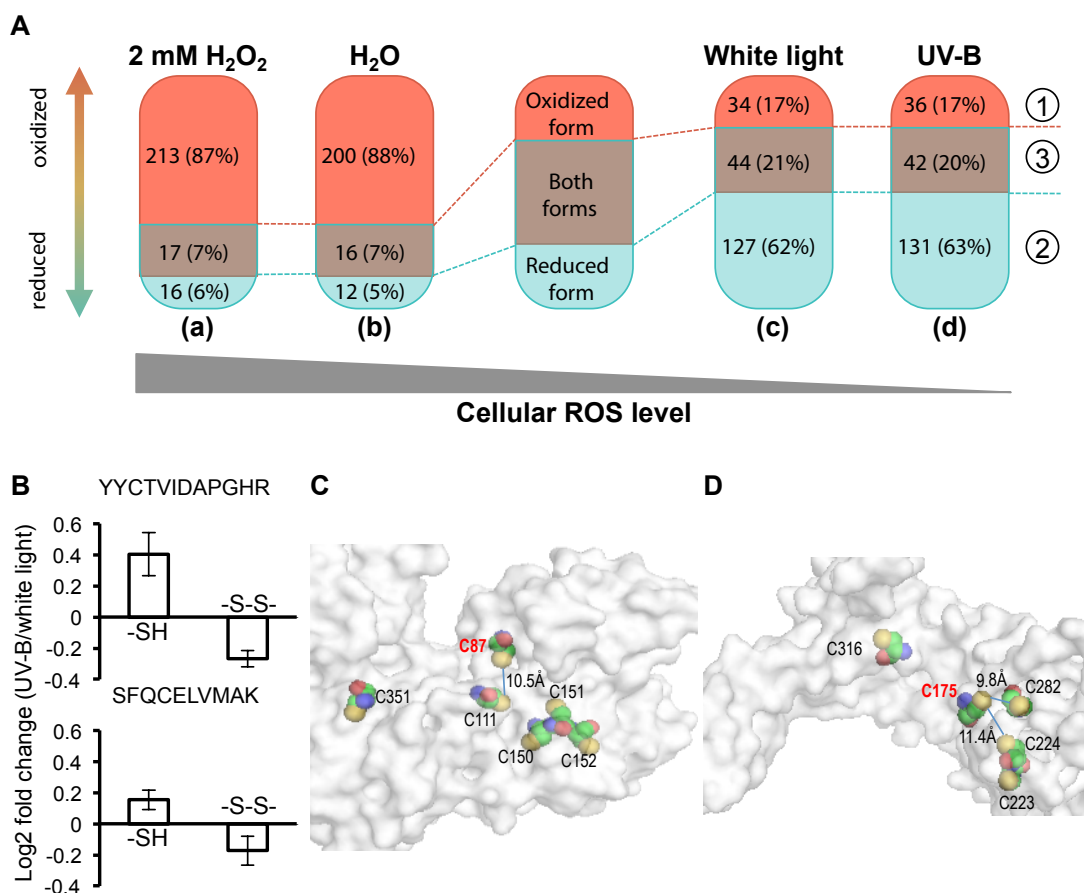


**Figure 4: Quantitative and differential thiol redox proteomics performed on reduction rich plant.**

(A) represents the numbers of peptides identified from samples with different treatments: 10-min H<sub>2</sub>O<sub>2</sub> treatment (a), 10-min deionized water treatment (b), 15-min white light treatment (c), and 15-min UV-B treatment (d). Index 1, 2 and 3 in circle represents the peptides detected in reduced (MPB-labeled), oxidized (BIAM-labeled) and both reduced and oxidized (both MPB- and BIAM-labeled) forms, respectively.

(B) shows the redox state changes of two independent redox-sensitive cysteine-containing peptides from both MPB- and BIAM-labeled experiments. YYCTVIDAPGHR and <sup>172</sup>SFQCELVMAK is derived from GTP binding Elongation factor Tu family proteins (AT1G07920, AT1G07930, AT1G07940 or AT5G60390) and RuBisCO activase (RCA, AT2G39730), respectively.

(C) and (D) represents the 3-D structure of aa2-aa431 region of GTP binding Elongation factor Tu family protein (AT1G07920) and aa123-aa415 region of RCA, respectively. The structures are depicted by ESyPred3D program, in which all cysteine residues are highlighted with the colored atoms: Green stands for carbon, red for oxygen, blue for nitrogen and yellow for sulfur, respectively. Cysteines reduced by 15-min UV-B exposure, i.e. C87 of GTP binding Elongation factor Tu family protein (AT1G07920) and C175 of RCA, are annotated in red. The distances between these two residues and their closest cysteines are indicated, with which the intra-molecular disulfide bridges may form between the sulfide atoms linked by blue bars when conformation changes.

the only cysteine residue present in plant CaM proteins, C27 is in fact substituted by threonine, glutamine or serine residue in CaM proteins of other organisms [81,83]. Having said these, it is still unclear that how C27 is involved in Ca<sup>2+</sup> co-ordination and/or protein binding. Based on the study from other kingdoms of organisms, CaM does not have any effects on catalases [84]. However, It is possible that CaM has a dual effect on regulation of H<sub>2</sub>O<sub>2</sub> level i.e. CaM stimulates hydrogen peroxide production via CaM-dependent NAD kinase activities [85], and, at the same time, down-regulates hydrogen peroxide level via increasing the activities of plant catalase [84]. Though higher chance of false positive results may be found from the list generated according to student's t-test alone, a tradeoff will be that these interesting candidates identified by a less stringent method may be worthy of pursuing further.

Oxidized forms of C208 and C218 of Bifunctional inhibitor/lipid-transfer protein/seed storage 2S albumin superfamily protein

(AT2G10940) increased in H<sub>2</sub>O<sub>2</sub>-treated plants. Albeit the function of this protein is largely unknown, bioinformatics prediction through the Protein Model Portal (PMP) in the Protein Structure Initiative (PSI) (<http://www.proteinmodelportal.org/>) has shown that these two residues can form intramolecular disulfide bonds with other cysteine residues (Supplementary Figure 3, illustrated by ESyPred3D program [86]). Thus, oxidation of these residues may cause conformation change that can affect activity and/or stability of the protein. As a lipid-transfer protein, modifications on cysteine residues identified from our data suggest that it may play a role in ROS-triggered lipid peroxidation. In addition, it has been reported that disulfide bond is formed between the RBCS subunit proteins [87]. Although the pairwise distance between any two of all four cysteine residues in the protein are relatively large [88], the disulfide bond can be formed through some conformational change. The distances between C96 and C132 (10.3 Å) and C96 and

C145 (11.9 Å), which were altered by H<sub>2</sub>O<sub>2</sub>, are the shortest two within all pairwise distances of cysteines in RBCS1B based on the 3-D structure predicted by PMP (Supplementary Figure 4, [86]). Thus, it is likely that the formation of intramolecular disulfide bridge may form between the cysteine residues detected, suggesting that *OxNSIL* may detect the disulfide bridge in an unbiased fashion.

### Substantiation of *OxNSIL* with a reduction-rich cellular environment in *Arabidopsis*

To further validate the effectiveness of *OxNSIL*, the thiol redox states in ambient UV-B radiation-treated *Arabidopsis* were further investigate using this approach because it has recently been reported that Atypical Cys His Rich Thioredoxin 1 (ACHT1), a thylakoid-associated atypical thioredoxin-type protein, is transiently reduced by photosynthetic reducing equivalents when the dark-adapted *Arabidopsis* was illuminated with a light of moderate intensity before this protein is eventually oxidized by the light-induced ROS [89]. Inspired by this finding, 3-week old white light-grown *Arabidopsis* plants illuminated by a short-term ambient UV-B irradiation were compared to that grown in white light. As expected, unlike results from H<sub>2</sub>O<sub>2</sub>-treatment experiment, more reduced forms of redox-sensitive peptides were detected. Totally, there were 78 BIAM-labeled peptides and 171 MPB-labeled identified from 6 groups of the control white-light-grown *Arabidopsis*, whereas there were 78 BIAM-labeled peptides and 173 MPB-labeled found from 6 groups of UV-B radiation-treated plants repetitively (Figure 4A). Moreover, quantitative thiol redox proteomic analyses have shown that 11 significantly altered peptides were in fact reduced (*i.e.* 9 reduced isoforms increased and 2 oxidized isoforms decreased) whereas only 2 were oxidized (*i.e.* 1 reduced isoform decreased and 1 oxidized isoform decreased) in the UV-B light-treated plants as compared to that grown in white light (Supplementary Figure 5). These results are consistent with previous founding that the most proteins are in reduced forms under normal conditions [13]. Moreover, unlike extremely oxidized states observed from the H<sub>2</sub>O<sub>2</sub>-treated plants, opposite changes (*i.e.* increase in its oxidized form and decrease in its reduced form or *vice versa*) were observed for ROS-sensitive and thiol-containing peptides from UV-B-treated samples, including peptides SFQCELVMAK (derived from RCA) and YYCTVIDAPGHR (derived from GTP binding elongation factor Tu family proteins) (Figure 4B). In both cases, the oxidized form (BIAM-labeled) of PTM peptide decreased as its reduced form (MPB-labeled) increased (Figure 4B). Three-dimensional structures (Figures 4C and 4D) of these two proteins were predicted using the Protein Model Portal (PMP) in the Protein Structure Initiative (PSI) (<http://www.proteinmodelportal.org/>) and visualized by ESyPred3D program [86], which may participate in formation of intra-molecular disulfide bond formation. As it has been known that regulation of gene expression is controlled by alterations in cellular redox states triggered by either biotic or abiotic elicitors, labeling of both reduced and oxidized forms of thiol group from one experiment provides more comprehensive site-specific thiol redox information and reveals the post-translational regulation independent of transcriptional control. Taking together, the *OxNSIL* approach is able to capture the intracellular redox states of protein cysteines, indicating that *in vivo* thiol redox states are not, or only slightly affects by our procedure.

### Conclusion

*OxNSIL* was designed to integrate advantages of biotin-tagged thiol-reactive reagents chemical labeling with that of <sup>15</sup>N stable isotope metabolic labeling to develop a high-throughput differential

and quantitative thiol redox proteomic approach. The biotin-tagged alkylating reagent is a widely used thiol-reactive reagent since it provides an advantage to the affinity purification for cysteine thiol-containing peptides and for deep sequencing of redox proteome of plants. Given the stable isotope metabolic labeling has been successfully applied to characterize the PTM in numerous proteomics studies [32,34,62], the heavy nitrogen-based stable isotope metabolic labeling strategy is hereby employed, which utilizes the autotrophic feature of plants that can grow on heavy nitrogen-coded salt medium as a cheaper way of protein labeling. As compared to the 2DE-based redox proteomics in response to various oxidative stresses [90], which have the advantage to provide a visual representation of the results, the MS-based approach focuses on the site-specific, comprehensive and quantitative study of oxidative and/or reductive alterations of any cysteine-containing proteins. The strategies of *OxICAT* and *OxMRM*, which are different from *ICAT*, *CysTMT*, *CysTRAQ*, and *OxiTRAQ* that aim to quantify the reduced or oxidized cysteine in two samples, are suitable to differentially label the reduced and oxidized forms of cysteines in a single sample and monitor the ratios of oxidized and reduced isoforms directly. On the other hand, the potential artifacts caused by chemical labeling variation using stable isotope tags can be avoided in the stable isotope metabolic labeling. Albeit the *SILAC*-based quantitative proteomics approaches have been applied to study the alteration of S-nitrosoproteins with the advantage of labeling the control and treated samples at the initial stage with amino acids, *OxNSIL* strategy offers a more convenient and economical way to study thiol redox in autotrophic organisms relying both photosynthesis to assimilate carbon and nitrogen stable isotope-coded salt to grow. In our approach, independent quantitative proteomic analyses of both reduced and reversibly oxidized cysteine residues have been performed in parallel, which not only saves time and reduces cost, but also avoids the potential variations resulting from differential labeling of peptides performed in different experimental procedures.

To obtain a proof-of-concept result, the analysis of 10-min H<sub>2</sub>O<sub>2</sub>-treated plants has confirmed that it is a powerful tool in identifying thiol redox proteome in plant and in quantifying site-specific thiol redox isoforms of proteins. Although only hundreds of peptides were detected in this experiment, a better improvement in redox peptide identification is expected if the labeled redox-peptides were further fractionated *via* multidimensional protein identification technology (MudPIT) and a newer version of MS machine would be used for analysis. The experimental cost used on identification and quantification of each redox peptide can be substantially reduced. Since ROS plays multiple and diverse roles in cellular events, such as induction of DNA/protein damages and as a second messenger of signaling, studies on the redox altered PTM of proteins have become essential in understanding of pathogen resistance stress response, hormonal response and other external regulators such as gravity, Nod factors or phytotoxins, the *OxNSIL* should become a powerful approach in discovering the redox-sensitive proteins involved in the key cellular processes and reveal the role of redox alteration in the regulation of plant growth and development and its adaptation to stresses.

### Acknowledgement

This work was supported by grants 661613, CAS10SC01, HKUST10/CRF/10, HKUST12/CRF/11G, GMGS14SC01, NMESL11SC01, PD13SC01, the National Natural Science Foundation of China (Grant No. 31370315) and internal supports from the CAS/HKUST joint laboratory and the School of Science Bioenergy program of HKUST.

## References

- Møller IM, Jensen PE, Hansson A (2007) Oxidative modifications to cellular components in plants. *Annu Rev Plant Biol* 58: 459-481.
- Pitzschke A, Forzani C, Hirt H (2006) Reactive oxygen species signaling in plants. *Antioxid Redox Signal* 8: 1757-1764.
- Potters G, Horemans N, Jansen MA (2010) The cellular redox state in plant stress biology—a charging concept. *Plant Physiol Biochem* 48: 292-300.
- Mikkelsen RB, Wardman P (2003) Biological chemistry of reactive oxygen and nitrogen and radiation-induced signal transduction mechanisms. *Oncogene* 22: 5734-5754.
- Kunsch C, Medford RM (1999) Oxidative stress as a regulator of gene expression in the vasculature. *Circ Res* 85: 753-766.
- Stamler JS, Lamas S, Fang FC (2001) Nitrosylation: the prototypic redox-based signaling mechanism. *Cell* 106: 675-683.
- Georgiou G (2002) How to flip the (redox) switch. *Cell* 111: 607-610.
- Davies MJ, Fu S, Wang H, Dean RT (1999) Stable markers of oxidant damage to proteins and their application in the study of human disease. *Free Radic Biol Med* 27: 1151-1163.
- Rinalducci S, Murgiano L, Zolla L (2008) Redox proteomics: basic principles and future perspectives for the detection of protein oxidation in plants. *J Exp Bot* 59: 3781-3801.
- Bachi A, Dalle-Donne I, Scaloni A (2013) Redox proteomics: chemical principles, methodological approaches and biological/biomedical promises. *Chem Rev* 113: 596-698.
- Mann M, Jensen ON (2003) Proteomic analysis of post-translational modifications. *Nat Biotechnol* 21: 255-261.
- Witze ES, Old WM, Resing KA, Ahn NG (2007) Mapping protein post-translational modifications with mass spectrometry. *Nat Methods* 4: 798-806.
- Foyer CH, Noctor G (2005) Redox homeostasis and antioxidant signaling: a metabolic interface between stress perception and physiological responses. *Plant Cell* 17: 1866-1875.
- Hwang C, Sinskey AJ, Lodish HF (1992) Oxidized redox state of glutathione in the endoplasmic reticulum. *Science* 257: 1496-1502.
- Jensen KS, Hansen RE, Winther JR (2009) Kinetic and thermodynamic aspects of cellular thiol-disulfide redox regulation. *Antioxid Redox Signal* 11: 1047-1058.
- Thamsen M, Jakob U (2011) The redoxome: Proteomic analysis of cellular redox networks. *Curr Opin Chem Biol* 15: 113-119.
- Beer SM, Taylor ER, Brown SE, Dahm CC, Costa NJ, et al. (2004) Glutaredoxin 2 catalyzes the reversible oxidation and glutathionylation of mitochondrial thiol proteins: implications for mitochondrial redox regulation and antioxidant DEFENSE. *J Biol Chem* 279: 47939-47951.
- Shelton MD, Chock PB, Mieyal JJ (2005) Glutaredoxin: role in reversible protein s-glutathionylation and regulation of redox signal transduction and protein translocation. *Antioxid Redox Signal* 7: 348-366.
- Chen XY, Wang SM, Li N, Hu Y, Zhang Y, et al. (2013) Creation of lung-targeted dexamethasone immunoliposome and its therapeutic effect on bleomycin-induced lung injury in rats. *PLoS One* 8: e58275.
- Mansoor MA, Svardal AM, Schneede J, Ueland PM (1992) Dynamic Relation between Reduced, Oxidized, and Protein-Bound Homocysteine and Other Thiol Components in Plasma during Methionine Loading in Healthy-Men. *Clin Chem* 38: 1316-1321.
- Ghezzi P, Bonetto V (2003) Redox proteomics: identification of oxidatively modified proteins. *Proteomics* 3: 1145-1153.
- Leichert LI, Jakob U (2004) Protein thiol modifications visualized in vivo. *PLoS Biol* 2: e333.
- Wang H, Wang S, Lu Y, Alvarez S, Hicks LM, et al. (2012) Proteomic analysis of early-responsive redox-sensitive proteins in *Arabidopsis*. *J Proteome Res* 11: 412-424.
- Murray CI, Van Eyk JE (2012) Chasing cysteine oxidative modifications: proteomic tools for characterizing cysteine redox status. *Circ Cardiovasc Genet* 5: 591.
- Charles R, Jayawardhana T, Eaton P (2014) Gel-based methods in redox proteomics. *Biochim Biophys Acta* 1840: 830-837.
- Sommer A, Traut RR (1974) Diagonal polyacrylamide-dodecyl sulfate gel electrophoresis for the identification of ribosomal proteins crosslinked with methyl-4-mercaptobutyrimidate. *Proc Natl Acad Sci U S A* 71: 3946-3950.
- Chiappetta G, Ndiaye S, Igbaria A, Kumar C, Vinh J, et al. (2010) Proteome screens for Cys residues oxidation: the redoxome. *Methods Enzymol* 473: 199-216.
- Ficarro SB, McClelland ML, Stukenberg PT, Burke DJ, Ross MM, et al. (2002) Phosphoproteome analysis by mass spectrometry and its application to *Saccharomyces cerevisiae*. *Nat Biotechnol* 20: 301-305.
- Aebersold R, Mann M (2003) Mass spectrometry-based proteomics. *Nature* 422: 198-207.
- Lee K, Lee J, Kim Y, Bae D, Kang KY, et al. (2004) Defining the plant disulfide proteome. *Electrophoresis* 25: 532-541.
- McDonagh B, Ogueta S, Lasarte G, Padilla CA, Barcena JA (2009) Shotgun redox proteomics identifies specifically modified cysteines in key metabolic enzymes under oxidative stress in *Saccharomyces cerevisiae*. *J Proteomics* 72: 677-689.
- Kline KG, Barrett-Wilt GA, Sussman MR (2010) In planta changes in protein phosphorylation induced by the plant hormone abscisic acid. *Proc Natl Acad Sci U S A* 107: 15986-15991.
- McClatchy DB, Liao L, Park SK, Xu T, Lu B, et al. (2011) Differential proteomic analysis of mammalian tissues using SILAM. *PLoS One* 6: e16039.
- Yu Y, Yoon SO, Poulougiannis G, Yang Q, Ma XM, et al. (2011) Phosphoproteomic analysis identifies Grb10 as an mTORC1 substrate that negatively regulates insulin signaling. *Science* 332: 1322-1326.
- Gygi SP, Rist B, Gerber SA, Turecek F, Gelb MH, et al. (1999) Quantitative analysis of complex protein mixtures using isotope-coded affinity tags. *Nat Biotechnol* 17: 994-999.
- Sethuraman M, McComb ME, Heibeck T, Costello CE, Cohen RA (2004) Isotope-coded affinity tag approach to identify and quantify oxidant-sensitive protein thiols. *Mol Cell Proteomics* 3: 273-278.
- Hägglund P, Bunkenborg J, Maeda K, Svensson B (2008) Identification of thioredoxin disulfide targets using a quantitative proteomics approach based on isotope-coded affinity tags. *J Proteome Res* 7: 5270-5276.
- Fu C, Wu C, Liu T, Ago T, Zhai P, et al. (2009) Elucidation of thioredoxin target protein networks in mouse. *Mol Cell Proteomics* 8: 1674-1687.
- Leichert LI, Gehrke F, Gudiseva HV, Blackwell T, Ilbert M, et al. (2008) Quantifying changes in the thiol redox proteome upon oxidative stress in vivo. *Proc Natl Acad Sci U S A* 105: 8197-8202.
- Tambor V, Hunter CL, Seymour SL, Kacerovsky M, Stulik J, et al. (2012) CysTRAQ - A combination of iTRAQ and enrichment of cysteinyl peptides for uncovering and quantifying hidden proteomes. *J Proteomics* 75: 857-867.
- Liu P, Zhang H, Wang H, Xia Y (2014) Identification of redox-sensitive cysteines in the *Arabidopsis* proteome using OxiTRAQ, a quantitative redox proteomics method. *Proteomics* 14: 750-762.
- Parker J, Zhu N, Zhu M, Chen S (2012) Profiling thiol redox proteome using isotope tagging mass spectrometry. *J Vis Exp*.
- Held JM, Danielson SR, Behring JB, Atsriku C, Britton DJ, et al. (2010) Targeted quantitation of site-specific cysteine oxidation in endogenous proteins using a differential alkylation and multiple reaction monitoring mass spectrometry approach. *Mol Cell Proteomics* 9: 1400-1410.
- Martínez-Acedo P, Núñez E, Gómez FJ, Moreno M, Ramos E, et al. (2012) A novel strategy for global analysis of the dynamic thiol redox proteome. *Mol Cell Proteomics* 11: 800-813.
- Bantscheff M, Schirle M, Sweetman G, Rick J, Kuster B (2007) Quantitative mass spectrometry in proteomics: a critical review. *Anal Bioanal Chem* 389: 1017-1031.
- Thompson JW, Forrester MT, Moseley MA, Foster MW (2013) Solid-phase capture for the detection and relative quantification of S-nitrosoproteins by mass spectrometry. *Methods* 62: 130-137.
- Chouchani ET, James AM, Fearnley IM, Lilley KS, Murphy MP (2011)

- Proteomic approaches to the characterization of protein thiol modification. *Curr Opin Chem Biol* 15: 120-128.
48. Guo G, Li N (2011) Relative and accurate measurement of protein abundance using <sup>15</sup>N stable isotope labeling in *Arabidopsis* (SILIA). *Phytochemistry* 72: 1028-1039.
49. Slesak I, Libik M, Karpinska B, Karpinski S, Miszalski Z (2007) The role of hydrogen peroxide in regulation of plant metabolism and cellular signalling in response to environmental stresses. *Acta Biochim Pol* 54: 39-50.
50. Hung SH, Yu CW, Lin CH (2005) Hydrogen peroxide functions as a stress signal in plants. *Bot Bull Acad Sinica* 46: 1-10.
51. Wan XY, Liu JY (2008) Comparative proteomics analysis reveals an intimate protein network provoked by hydrogen peroxide stress in rice seedling leaves. *Mol Cell Proteomics* 7: 1469-1488.
52. Li H, Wong WS, Zhu L, Guo HW, Ecker J, et al. (2009) Phosphoproteomic analysis of ethylene-regulated protein phosphorylation in etiolated seedlings of *Arabidopsis* mutant *ein2* using two-dimensional separations coupled with a hybrid quadrupole time-of-flight mass spectrometer. *Proteomics* 9: 1646-1661.
53. Jain S, McGinnes LW, Morrison TG (2007) Thiol/disulfide exchange is required for membrane fusion directed by the Newcastle disease virus fusion protein. *J Virol* 81: 2328-2339.
54. Li S, Whorton AR (2003) Regulation of protein tyrosine phosphatase 1B in intact cells by S-nitrosothiols. *Arch Biochem Biophys* 410: 269-279.
55. Skalska J, Brookes PS, Nadochiy SM, Hilchey SP, Jordan CT, et al. (2009) Modulation of cell surface protein free thiols: a potential novel mechanism of action of the sesquiterpene lactone parthenolide. *PLoS One* 4: e8115.
56. Harris C, Shuster DZ, Roman Gomez R, Sant KE, Reed MS, et al. (2013) Inhibition of glutathione biosynthesis alters compartmental redox status and the thiol proteome in organogenesis-stage rat conceptuses. *Free Radic Biol Med* 63: 325-337.
57. Rogers LK, Leinweber BL, Smith CV (2006) Detection of reversible protein thiol modifications in tissues. *Anal Biochem* 358: 171-184.
58. Dennehy MK, Richards KA, Wernke GR, Shyr Y, Liebler DC (2006) Cytosolic and nuclear protein targets of thiol-reactive electrophiles. *Chem Res Toxicol* 19: 20-29.
59. Lamesch P, Berardini TZ, Li D, Swarbreck D, Wilks C, et al. (2012) The *Arabidopsis* Information Resource (TAIR): improved gene annotation and new tools. *Nucleic Acids Res* 40: D1202-D1210.
60. Shen BQ, Xu KY, Liu LN, Raab H, Bhakta S, et al. (2012) Conjugation site modulates the in vivo stability and therapeutic activity of antibody-drug conjugates. *Nat Biotechnol* 30: 184-189.
61. Kalia J, Raines RT (2007) Catalysis of imido group hydrolysis in a maleimide conjugate. *Bioorg Med Chem Lett* 17: 6286-6289.
62. Yang Z, Guo G, Zhang M, Liu CY, Hu Q, et al. (2013) Stable isotope metabolic labeling-based quantitative phosphoproteomic analysis of *Arabidopsis* mutants reveals ethylene-regulated time-dependent phosphoproteins and putative substrates of constitutive triple response 1 kinase. *Mol Cell Proteomics* 12: 3559-3582.
63. Li L, Kresh JA, Karabacak NM, Cobb JS, Agar JN, et al. (2008) A hierarchical algorithm for calculating the isotopic fine structures of molecules. *J Am Soc Mass Spectrom* 19: 1867-1874.
64. Benjamini Y, Hochberg Y (1995) Controlling the False Discovery Rate - a Practical and Powerful Approach to Multiple Testing. *J Roy Stat Soc B Met* 57: 289-300.
65. Winther JR, Thorpe C (2014) Quantification of thiols and disulfides. *Biochim Biophys Acta* 1840: 838-846.
66. Gallogly MM, Starke DW, Miesal JJ (2009) Mechanistic and kinetic details of catalysis of thiol-disulfide exchange by glutaredoxins and potential mechanisms of regulation. *Antioxid Redox Signal* 11: 1059-1081.
67. Ellis RJ (1979) Most Abundant Protein in the World. *Trends Biochem Sci* 4: 241-244.
68. Yu J, Chen S, Wang T, Sun G, Dai S (2013) Comparative Proteomic Analysis of *Puccinellia tenuiflora* Leaves under Na<sub>2</sub>CO<sub>3</sub> Stress. *Int J Mol Sci* 14: 1740-1762.
69. Peck SC (2005) Update on proteomics in *Arabidopsis*. Where do we go from here? *Plant Physiol* 138: 591-599.
70. Abraham P, Giannone RJ, Adams RM, Kalluri U, Tuskan GA, et al. (2013) Putting the pieces together: high-performance LC-MS/MS provides network-, pathway-, and protein-level perspectives in *Populus*. *Mol Cell Proteomics* 12: 106-119.
71. Bykova NV, Rampitsch C (2013) Modulating protein function through reversible oxidation: Redox-mediated processes in plants revealed through proteomics. *Proteomics* 13: 579-596.
72. Fares A, Rossignol M, Peltier JB (2011) Proteomics investigation of endogenous S-nitrosylation in *Arabidopsis*. *Biochem Biophys Res Commun* 416: 331-336.
73. Romero-Puertas MC, Camprostrini N, Mattè A, Righetti PG, Perazzolli M, et al. (2008) Proteomic analysis of S-nitrosylated proteins in *Arabidopsis thaliana* undergoing hypersensitive response. *Proteomics* 8: 1459-1469.
74. Cohen I, Knopf JA, Irihimovitch V, Shapira M (2005) A proposed mechanism for the inhibitory effects of oxidative stress on Rubisco assembly and its subunit expression. *Plant Physiol* 137: 738-746.
75. Moreno J, García-Murria MJ, Marín-Navarro J (2008) Redox modulation of Rubisco conformation and activity through its cysteine residues. *J Exp Bot* 59: 1605-1614.
76. Marri L, Zaffagnini M, Collin V, Issakidis-Bourguet E, Lemaire SD, et al. (2009) Prompt and easy activation by specific thioredoxins of calvin cycle enzymes of *Arabidopsis thaliana* associated in the GAPDH/CP12/PRK supramolecular complex. *Mol Plant* 2: 259-269.
77. Wong JH, Cai N, Balmer Y, Tanaka CK, Vensel WH, et al. (2004) Thioredoxin targets of developing wheat seeds identified by complementary proteomic approaches. *Phytochemistry* 65: 1629-1640.
78. van der Linde K, Gutsche N, Leffers HM, Lindermayr C, Müller B, et al. (2011) Regulation of plant cytosolic aldolase functions by redox-modifications. *Plant Physiol Biochem* 49: 946-957.
79. De Laurentiis EI, Mo F, Wieden HJ (2011) Construction of a fully active Cys-less elongation factor Tu: functional role of conserved cysteine 81. *Biochim Biophys Acta* 1814: 684-692.
80. Kocsy G, Tari I, Vanková R, Zechmann B, Gulyás Z, et al. (2013) Redox control of plant growth and development. *Plant Sci* 211: 77-91.
81. Jeandroz S, Lamotte O, Astier J, Rasul S, Trapet P, et al. (2013) There's more to the picture than meets the eye: nitric oxide cross talk with Ca<sup>2+</sup> signaling. *Plant Physiol* 163: 459-470.
82. Perochon A, Aldon D, Galaud JP, Ranty B (2011) Calmodulin and calmodulin-like proteins in plant calcium signaling. *Biochimie* 93: 2048-2053.
83. Zielinski RE (1998) Calmodulin and Calmodulin-Binding Proteins in Plants. *Annu Rev Plant Physiol Plant Mol Biol* 49: 697-725.
84. Yang T, Poovaiah BW (2002) Hydrogen peroxide homeostasis: activation of plant catalase by calcium/calmodulin. *Proc Natl Acad Sci U S A* 99: 4097-4102.
85. Harding SA, Oh SH, Roberts DM (1997) Transgenic tobacco expressing a foreign calmodulin gene shows an enhanced production of active oxygen species. *EMBO J* 16: 1137-1144.
86. Lambert C, Léonard N, De Bolle X, Depiereux E (2002) ESyPred3D: Prediction of proteins 3D structures. *Bioinformatics* 18: 1250-1256.
87. Motohashi K, Kondoh A, Stumpp MT, Hisabori T (2001) Comprehensive survey of proteins targeted by chloroplast thioredoxin. *Proc Natl Acad Sci U S A* 98: 11224-11229.
88. Richardson JS (1981) The anatomy and taxonomy of protein structure. *Adv Protein Chem* 34: 167-339.
89. Dangoor I, Peled-Zehavi H, Wittenberg G, Danon A (2012) A chloroplast light-regulated oxidative sensor for moderate light intensity in *Arabidopsis*. *Plant Cell* 24: 1894-1906.
90. Tian S, Qin G, Li B (2013) Reactive oxygen species involved in regulating fruit senescence and fungal pathogenicity. *Plant Mol Biol* 82: 593-602.